JOURNAL OF MECHANICAL ENGINEERING AND SCIENCES
ISSN: 2289-4659 e-ISSN: 2231-8380
VOLUME 19, ISSUE 1, 2025, 10544 - 10553
DOI: https://doi.org/10.15282/jmes.19.1.2025.9.0826

RESEARCH ARTICLE

Effect of PVA/Col/HNT hydrogel on physiochemical properties of PVDF/PVA electrospun using casting and freeze-thawing method for nerve tissue regeneration application

M. S. A. Hamzah[1], N. H. M. Nayan[1,2]*, S. C. Fhong[3], N. Jusoh[4]

[1] Faculty of Engineering Technology, Universiti Tun Hussein Onn Malaysia, HKM 1 Hab Pendidikan Tinggi Pagoh, Jalan Panchor, 84600 Pagoh, Johor, Malaysia

[2] Research Centre for Applied Electromagnetic (EMC), Institute of Integrated Engineering (I2E), Universiti Tun Hussein Onn Malaysia, 86400 Parit Raja, Johor, Malaysia

Phone: +6069742032, Fax.: +6069742140

[3] Microelectronics and Nanotechnology-Shamsuddin Research Centre (MiNT-SRC), Institute of Integrated Engineering (I2E), Universiti Tun Hussein Onn Malaysia, 86400 Parit Raja, Johor, Malaysia

[4] Medical Device & Technology Centre (MEDITEC), Faculty of Electrical Engineering, Universiti Teknologi Malaysia, 81310 Johor Bharu, Johor, Malaysia

ABSTRACT - Nerve tissue engineering requires biomaterials that provide mechanical strength, biocompatibility, and an optimal microenvironment for cell attachment and proliferation. Electrospun polymeric scaffolds have gained attention due to their structural similarity to the extracellular matrix. However, their inherent brittleness and limited bioactivity necessitate further enhancement. This study investigates the effects of incorporating a polyvinyl alcohol/collagen/halloysite nanotube (PVA/Col/HNT) hydrogel on the physicochemical properties of polyvinylidene fluoride/polyvinyl alcohol (PVDF/PVA) electrospun mats to improve their suitability for nerve regeneration applications. The hydrogel was integrated onto the electrospun matrices using casting and freeze-thawing techniques. The resultant composites were characterized for their morphological, mechanical, and biological properties. Field emission scanning electron microscopy revealed a uniform distribution and interconnectivity between the electrospun mat and hydrogel layer, supported by Fourier transform infrared spectroscopy spectra indicating strong hydrogen bonding interactions. Atomic force microscopy demonstrated reduced surface roughness (R_a: 5.3 nm electrospun surface, 41.9 nm hydrogel surface) compared to single-layer electrospun mats (R_a: 192.5 nm), promoting better cell attachment and proliferation. Mechanical testing showed a significant increase in tensile strength (1.762 MPa) and Young's modulus (39.612 MPa) while maintaining high elongation at break (316.253%), ensuring flexibility and durability. The scaffold's piezoelectric properties further enhanced its potential for nerve regeneration. In vitro biocompatibility assays using human fibroblast cells confirmed increased cell adhesion and proliferation, highlighting the suitability of the PVA/Col/HNT hydrogel-infused PVDF/PVA mats for soft tissue engineering. This study underscores the composite's potential in advancing nerve regeneration therapies.

ARTICLE HISTORY
Received : 20th Oct. 2024
Revised : 25th Feb. 2025
Accepted : 05th Mar. 2025
Published : 30th Mar. 2025

KEYWORDS
Electrospinning
Freeze – thawing
Casting
Nerve tissue
Tissue regeneration
Bilayer composite

1. INTRODUCTION

The peripheral nervous system can regenerate and repair, but injuries are more common due to direct mechanical trauma. Regeneration capacity depends on the patient's age, injury mechanism, and proximity to the nerve cell body. Peripheral nerve injuries are uncommon, affecting only 3% of severe injuries [1, 2]. Direct nerve restoration with autografts is the gold standard for severe axonotmesis and neurotmesis injuries. However, autografts have drawbacks such as inadequate donor tissue availability, secondary incisions, loss of feeling, potential neuroma formation, and less-than-ideal donor nerve dimensions [3, 4]. To address these issues, tissue engineering has created artificial nerve grafts. In peripheral nerve surgery, tissue engineering research focuses primarily on recreating and repairing the end of the nerve farthest from the lesion site after a peripheral nerve injury [5-7]. An ideal nerve substitute would comprise a scaffold component that replicates the extracellular matrix of the peripheral nerve, together with a cellular component that promotes and sustains the regeneration of peripheral nerve axons [8]. The scaffold must possess the ability to enhance cell proliferation, enable the maintenance of specialized cell activities, and assist cell adhesion [8, 9].

The transmission of bioelectrical signals is crucial for the functional recovery of nerves, and an ideal peripheral nerve scaffold should have electrical activity properties similar to natural nerves [10]. Piezoelectric materials can convert stress changes into electrical signals, activating intracellular signaling pathways critical for cell activity and function [10, 11]. Polyvinylidene fluoride (PVDF) is a thermoplastic fluoropolymer chemically inert and synthesized through the

*CORRESPONDING AUTHOR | N. H. M. Nayan | ✉ nadirul@uthm.edu.my

polymerization of vinylidene fluoride. It possesses notable characteristics such as strong piezoelectric properties, chemical resistance, biocompatibility, and transparency. It is extensively utilized in biomedical applications such as biosensors, smart drug delivery systems, and tissue engineering [12]. PVDF has poor reactive side chains, causing nutrient transport and membrane wettability, which can cause inflammation and hinder drug carrier function [13, 14]. As a result, previous research used the Taguchi Method to investigate the influence of polyvinyl alcohol (PVA) on the physiochemical properties and biocompatibility of PVDF electrospun. PVA is a nontoxic, biocompatible, and biodegradable polymer for tissue engineering [15]. Incorporating PVA with other polymer solutions increases the free surface energy, allowing for high drug loading capacity and cell migration during healing processes. The optimal PVDF/PVA electrospun fiber demonstrated good biocompatibility properties and a low toxic potential for human cells.

Despite the vast advantages of electrospinning in biomedical applications, the single design is less favorable due to its mechanical properties and high burst release effect. The bilayer or multilayer design provides considerable benefits over single-layer scaffolds in nerve tissue regeneration by creating a more biomimetic environment that improves cellular connections and functional recovery [16]. Research indicates that bilayer scaffolds incorporate varied material compositions and structures in separate layers to facilitate neuronal development and extracellular matrix deposition. A bilayer scaffold with an electrospun polycaprolactone (PCL) outer layer and a hydrogel-based inner layer exhibited enhanced mechanical support. It facilitated Schwann cell migration and axonal regeneration compared to single-layer structures [17]. In a rat sciatic nerve damage model, bilayer scaffolds with a gradient structure enhanced nerve conduction velocity and functional recovery scores by up to 35% compared to single-layer scaffolds [18, 19]. These findings underscore the significance of biomimetic stratification in scaffold design to improve peripheral nerve healing.

This study uses a bilayer conduit consisting of the electrospun layer and hydrogel layer structure that mimics the nerve tissue (axons, myelin sheath, and perineurium). This design allowed the conduit to release the therapeutic agents slowly over time. This kept the area clean while the patient healed, protected it from external mechanical stress, and helped cells adhesion and grow. The hydrogel was fabricated using PVA as the base material, which enhanced drug loading capacity and improved moisture absorption. The hydrogel layer also has halloysite nanotubes (HNT) and collagen, which help cells stick together. The HNT gives the nerve conduits a lot of surface area for drugs and cells to interact.

2. MATERIAL AND METHODS

2.1 Development of Bilayer Electrospun-Hydrogel Layer

The electrospun layer was formed by dissolving PVDF ($M_w \approx 534000$ g/mol) in dimethyl sulfoxide with PVA ($M_w \geq$ 89000 g/mol) at a PVDF-to-PVA ratio of 90:10 to form homogenous electrospinning solutions. As reported in previous work, as illustrated in Figure 1 [15, 20], the suspension was placed into a syringe and electrospun at 10 kV for 1 hour at 0.5 mL/h and 15 cm tip-to-collector distance under ambient conditions. The hydrogel solution was developed by dissolving PVA in distilled water, resulting in a 13% (w/v) solution, which was then modified with 3 wt% collagen (M_w = 300000 g/mol), and 2 wt% halloysite nanotube, HNT (M_w = 258 g/mol). Next, we placed the PVDF/PVA electrospun on top of a glass dish and filled it with PVA/Col/HNT hydrogel before proceeding with the casting process. The sample underwent freeze-thaw cycles three times to form an electrospun-hydrogel bilayer conduit film scaffold.

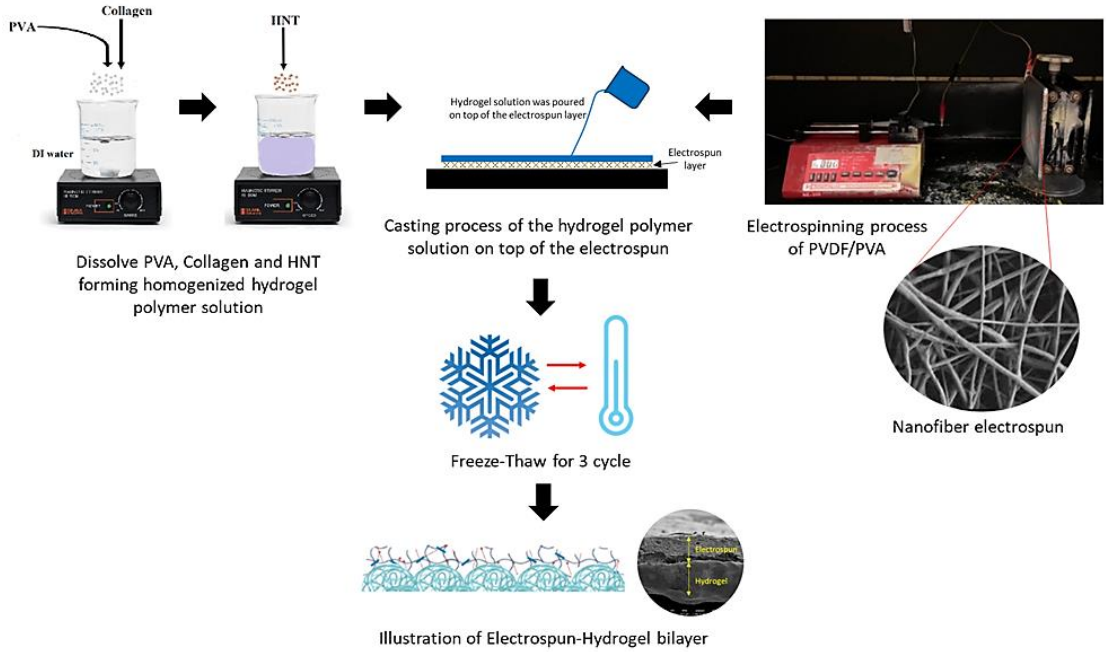

Figure 1. The development process of electrospun-hydrogel bilayer conduit films scaffold

2.2 Morphological Characterizations

Field Emission Scanning Electron Microscope (FESEM) was utilized for morphological observation of hydrogel coating on electrospun to form bilayer conduit film, with samples coated with gold for 30 seconds and examined at 500-10000X magnification using Image J software. Atomic Force Microscopy (AFM) uses a cantilever tip to image the sample, providing a highly high-resolution image of the surface topography of the sample structure. We prepared the samples to a size of 1 cm x 1 cm and used the AFM (Park System XE-100, Korea) in contact mode to measure the root mean square roughness of the scaffold sample, following ASTM E2859-11 [21] guidelines.

2.3 Mechanical Characterization – Tensile Testing

A tensile test was conducted on samples prepared according to ASTM D3039/D3039M [22]. The samples were pulled until they broke to measure ultimate tensile strength, Young modulus, and elongation at break. The ends were mounted with a gauge length of 15 mm, and the test was conducted at a strain rate of 10 mm/min and load strength of 5 kN at room temperature.

2.4 Chemical Characterization – Fourier Transform Infrared Spectroscopy Testing

A 1 cm × 1 cm composite was positioned in the sample holder, assuring coverage and alignment with the infrared spectroscopy source. Fourier Transform Infrared Spectroscopy (FTIR) (Perkin Elmer) was employed to ascertain the band value and existence resulting from the interaction between the bilayer composite. This study utilized a 4000-400 cm^{-1} range with a resolution of 4 cm^{-1} to analyze the primary functional groups.

2.5 Conductivity Analysis

A customized Faraday Bucket was used to detect the samples' surface charge potentials after they were sliced into 4 cm × 4 cm pieces [22, 23]. The voltage potential difference between the ground and the bucket was measured using a simple electrometer (PASCO Scientific). The electrometer's potential measurements were recorded approximately every 60 seconds.

2.5 Biological Analysis

Human Skin Fibroblast (HSF 1184) cells were cultivated in T-flasks using DMEM media enriched with fetal bovine serum, penicillin-streptomycin, and pyruvate, all sourced from Thermo Fisher Scientific. Before cytotoxicity examination, the cells were cultured at 37ºC with a CO_2 concentration of 5%. The sample was inoculated with a suspension of HSF cells at a concentration of $1x10^4$ cells/mL for 24 hours. The MTT (3-[4,5-dimethylthiazol-2-yl]-2,5 diphenyl tetrazolium bromide) assay measured the absorbance of purple formazan crystals, indicating the amount of viable cells after 24 hours. The absorbance was measured at 570 nm using a microplate reader. The cells undergo Trixton-X treatment as the positive control, while normal culturing is the negative control. The specimens were stained with the Live/Dead kit assay to evaluate the cells' viability, and the image was recorded using an inverted fluorescence microscope.

3. RESULTS AND DISCUSSION

3.1 Morphological Analysis

The cross-sectional structure of the electrospun (a), hydrogel (b), and bilayer (c–d) are shown in Figure 2 by FESEM images. As illustrated in Figure 2(a), the electrospun fiber diameter produces an average diameter of 171.60±1.2 nm and 89.5±2.1% porosity reported by previous work [16]. The electrospun layer (Figure 2(a)) was composed of numerous fibers arranged in a manner that made it strong under tension and allowed the nerve conduits to remain flexible. These mechanical properties are crucial in protecting the inner, more delicate hydrogel layer from external forces, thus maintaining the integrity of the regenerating nerve [9, 2, 26]. The freeze-thaw method coats the electrospun with a hydrogel layer, increasing the fine fiber diameter up to 165.7±0.4 nm, which is beneficial for mimicking the extracellular matrix and supporting cell adhesion and proliferation, as indicated in Table 1. Figure 2(c-d) showed that the casting and freeze-thaw process successfully fabricated the PVA/Collagen/Halloysite Nanotube hydrogels combined with electrospun PVDF/PVA, forming a bilayer structure. It shows that the layers were intact and penetrated each other, as indicated by the arrow line. Casting hydrogel onto electrospun layers creates an intimate contact, allowing the hydrogel to adhere to the fibers' porous surface structures. The bilayer scaffold has the highest porosity (96.27±2.3%), which is advantageous for cell infiltration, nutrient exchange, and waste removal. This is even higher than the PVA/HNT/Col hydrogel (94.11±1.1%) and PVDF/PVA electrospun scaffold (89.50±2.1%). Hydrogels, especially those made of polyvinyl alcohol, commonly undergo crosslinking using the freeze-thaw method [22]. This process creates a network structure, with ice crystals forming during freezing and melting upon thawing. This process also facilitates crosslinking between the electrospun layer and hydrogel, promoting stronger adhesion and potential hydrogen bonding [22, 27]. This synergistic effect of electrospun fibers and hydrogel creates a multi-scale porous structure. The electrospun layer provides interconnected micro- and nanopores, while the hydrogel enhances porosity by retaining water and preventing fiber packing. This combination improves cell infiltration, nutrient diffusion, and extracellular matrix deposition, making it ideal for nerve tissue regeneration.

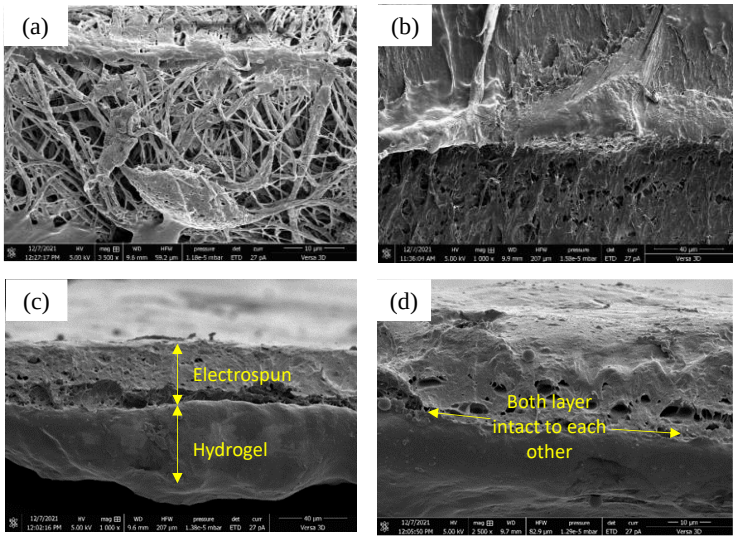

Figure 2. FESEM micrograph image of: (a) PVDF/PVA electrospun, (b) PVA/Collagen/HNT hydrogel and (c-d) electropsun/hydrogel bilayer cross-section

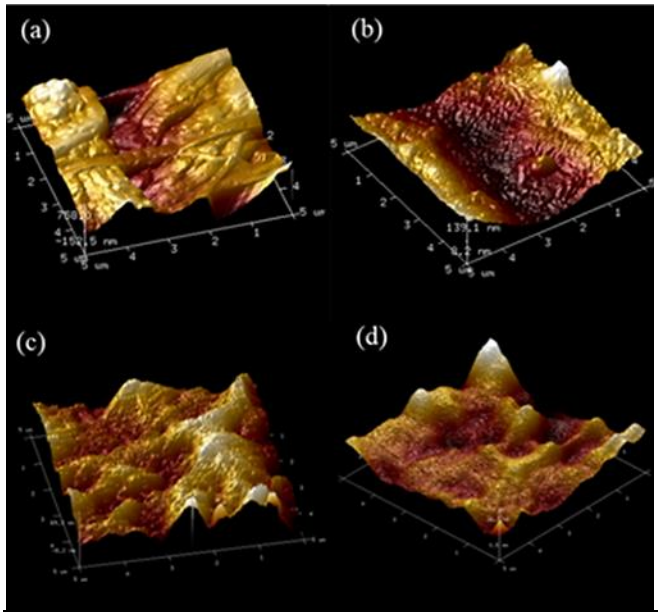

Sample	R_a (nm)	R_q (nm)
PVDF/PVA Electrospun	192.5±2.3	247.1±2.5
PVA/HNT/Col Hydrogel	78.8±1.5	95.4±1.8
Bilayer (Electrospun	5.3±2.8	7.5±1.1
Bilayer (Hydrogel Surface)	41.9±2.4	57.3±2.2

Figure 3. AFM images: (a) PVDF/PVA electrospun, (b) PVA/Collagen/HNT hydrogel and (c-d) electrospun/hydrogel bilayer cross-section as well as (e) the surface roughness of the surface

Table 1. Fiber diameter, porosity, thickness and sample potential per unit mass value of the composite scaffolds

Type of scaffolds	Fiber Diameter (nm)	Porosity (%)	Thickness	Sample potential per unit mass (V/g)
PVDF/PVA Electrospun	171.6±0.5	89.50±2.1	531.56±0.4 um	1.312±0.5
PVA/HNT/Col Hydrogel	-	94.11±1.1	0.092±0.2 mm	0.510±0.7
Electrospun – Hydrogel Bilayer	165.7±0.4	96.27±2.3	0.095±0.6 mm	0.892±0.1

The AFM micrograph in Figure 3 shows the PVDF/PVA nanofiber scaffold, the PVA/Collagen-HNT hydrogel scaffold, and the surface of the two-layer scaffold on both sides. The roughness of the surface can be qualitatively presented in average roughness, R_a, and root-mean-square roughness, Rq, where when the value of R_a and R_q increases, the roughness characteristic increases [28-30]. The samples' roughness values were in the nanoscale range, which

correlates to the high surface area that can enhance the attachment, growth, and proliferation of new nerve cells on the nerve scaffold [30]. The R_a and R_q values correlate with the porosity and morphological integrity of the scaffolds. The PVDF/PVA electrospun scaffold has the highest roughness (R_a: 192.5±2.3 nm, R_q: 247.1±2.5 nm), indicating a highly fibrous and irregular surface, which can enhance cell adhesion but may limit uniform cell growth. The PVA/HNT/Col hydrogel exhibits lower roughness (R_a: 78.8±1.5 nm, R_q: 95.4±1.8 nm), which aligns with its smoother, hydrated structure that supports cell proliferation. For the bilayer scaffold, the electrospun surface has the lowest roughness (R_a: 5.3±2.8 nm, R_q: 7.5±1.1 nm), suggesting a more compact and refined fiber arrangement, likely due to interaction with the hydrogel layer, reducing surface irregularities. Meanwhile, the hydrogel surface (R_a: 41.9±2.4 nm, R_q: 57.3±2.2 nm) shows moderate roughness, balancing surface smoothness for cell proliferation with sufficient texture for adhesion. These results align with the high porosity of the bilayer scaffold (96.27±2.3%), indicating an optimal microenvironment for nerve tissue regeneration by providing a structurally stable yet bioactive interface [31].

3.2 Mechanical Analysis

The mechanical properties of the electrospun-hydrogel bilayer scaffold demonstrate a significant improvement over single-layer scaffolds, balancing strength, flexibility, and elongation, which are crucial for nerve tissue regeneration. Table 2 shows that the PVDF/PVA electrospun has higher tensile strength than hydrogel due to its fibrous nature and tight packing. PVA/HNT/Col Hydrogel, a more flexible material, has lower tensile strength. The bilayer scaffold's tensile strength (1.762 MPa) is slightly higher than the electrospun scaffold (1.721 MPa) and significantly greater than the hydrogel (0.761 MPa), indicating that the integration of the hydrogel layer does not compromise structural integrity. The Young's modulus of the bilayer scaffold (39.612 MPa) is nearly 1.8 times higher than the electrospun scaffold (22.032 MPa) and 54 times higher than the hydrogel (0.725 MPa), suggesting that the bilayer design enhances rigidity while maintaining a controlled level of flexibility [32]. The electrospun has a high Young's modulus (22.032 MPa) but may lack flexibility in applications requiring adaptability, such as dynamic tissues like nerves. In comparison to other bilayer composite scaffolds, such as PCL/collagen or PLGA/gelatin bilayers, the electrospun-hydrogel bilayer exhibits superior elongation at break (316.253%), outperforming many reported bilayer systems where elongation often remains below 250% [33,34]. The electrospun-hydrogen bilayer exhibits the highest elongation at break (316.253%), making it a more ductile and stretchable material. Integrating the hydrogel into the electrospun fibers using the casting and freeze-thaw methods has resulted in a scaffold with a balance of mechanical strength, flexibility, and stretchability [32, 35].

Furthermore, the AFM roughness data correlates well with these findings—the lower roughness of the bilayer electrospun surface (R_a: 5.3 nm, R_q: 7.5 nm) suggests a smoother, more compact fiber arrangement, potentially enhancing mechanical strength. The hydrogel surface roughness (R_a: 41.9 nm, R_q: 57.3 nm) allows for better cell adhesion and migration, further improving scaffold performance. These results collectively highlight the bilayer system provides a suitable environment for cell attachment, migration, and proliferation. At the same time, its mechanical properties ensure that it can withstand the physical forces encountered in a biological system, particularly in nerve regeneration, where flexibility and mechanical support are critical [7, 8, 31].

Table 2. Mechanical analysis of the nerve tissue conduit scaffold

Type of scaffolds	Tensile strength (MPa)	Young Modulus (MPa)	Elongation at break (%)
PVDF/PVA Electrospun	1.721±0.661	22.032±0.504	28.281±0.051
PVA/HNT/Col Hydrogel	0.761±0.023	0.725±0.013	273.331±0.032
Electrospun – Hydrogel Bilayer	1.762±0.014	39.612±0.031	316.253±0.012

3.3 FTIR Analysis

The FTIR spectra of PVDF/PVA electrospun fibers, PVA/HNT/Collagen hydrogel, and the electrospun-hydrogel bilayer composite reveal distinct functional group interactions as indicated in Figure 4. In the PVDF/PVA electrospun spectrum, the presence of a broad peak around 3400 cm^{-1} indicates O-H stretching from PVA, while characteristic C-F stretching vibrations (~1170-880 cm^{-1}) confirm the presence of PVDF [16, 36]. The PVA/HNT/Collagen hydrogel spectrum shows a broad O-H stretching peak (~3300-3500 cm^{-1}) due to hydrogen bonding, along with amide I (~1650 cm^{-1}) and amide II (~1550 cm^{-1}) peaks, confirming collagen integration [37]. Additionally, Si-O stretching (~1000-1100 cm^{-1}) from HNT indicates its successful incorporation within the hydrogel network [22]. The electrospun-hydrogel bilayer spectrum combines key features of both individual components, maintaining a broad O-H stretching peak due to extensive hydrogen bonding while also exhibiting C-F stretching (~1170-880 cm^{-1}) from PVDF and Si-O peaks (~1000-1100 cm^{-1}) from HNT, demonstrating effective layer integration [36, 38]. The physical crosslinking in the bilayer is achieved through the freeze-thaw method, where repeated freezing induces ice crystal formation, forcing polymer chains closer together. Ice melting allows for strong intermolecular hydrogen bonds between PVA chains upon thawing, creating a stable hydrogel matrix [39]. This mechanism enhances the hydrogel's mechanical strength and structural integrity without requiring chemical crosslinking agents.

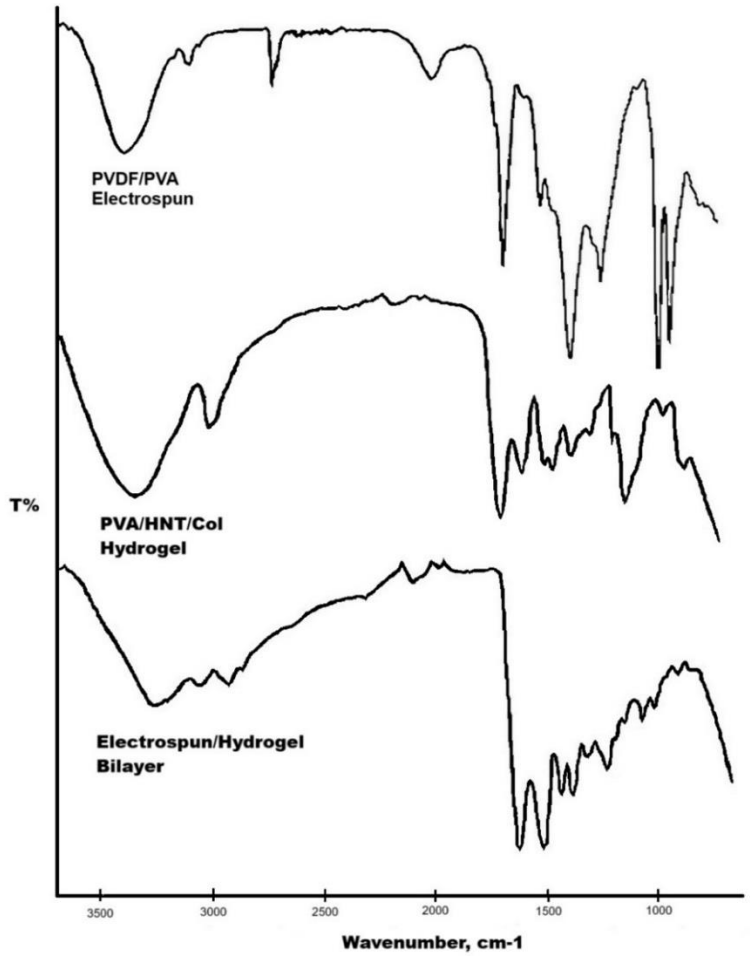

Figure 4. FTIR Spectra of electrospun, hydrogel, and bilayer composites

The electrospun layer interacts with the hydrogel via interfacial hydrogen bonding, primarily between PVA in both layers, ensuring strong adhesion. Hydrogen bonding in the electrospun-hydrogel bilayer composite can be verified by examining the large O-H stretching peak in the FTIR spectra. The O-H stretching band in the bilayer composite spectrum is about 3300–3400 cm^{-1}, resembling the hydrogel but exhibiting a more prominent profile and a minor shift relative to the individual components. This alteration and expansion signify improved hydrogen bond formation between PVA molecules in both layers (electrospun and hydrogel), demonstrating robust interfacial interactions. The amide I (~1650 cm^{-1}) and amide II (~1550 cm^{-1}) peaks from collagen are still prominent in the bilayer spectrum, indicating that hydrogen bonding between collagen (amide groups) and PVA (hydroxyl groups) enhances the composite's integrity. The Si-O stretching (~1000–1100 cm^{-1}) from HNT remains evident, suggesting that the nanotubes facilitate interfacial bonding through interacting with PVA hydroxyl groups. The primary evidence of hydrogen bonding in the bilayer composite is the lack of free hydroxyl peaks and the broad characteristic of the O-H band, indicating robust intermolecular hydrogen bonding instead of separate hydroxyl groups. The freeze-thaw process amplifies these interactions, resulting in the physical crosslinking essential for structural integrity. This verifies that the electrospun and hydrogel layers are effectively merged by hydrogen bonding rather than just physical adhesion.

3.4 Conductivity Analysis

The experimental findings indicate that PVDF/PVA electrospun fibers possess the maximum potential per unit mass at 1.312±0.5 V/g, followed by the electrospun-hydrogel bilayer composite at 0.892±0.1 V/g, and the PVA/HNT/Collagen hydrogel at 0.510±0.7 V/g as indicated in Table 1. These results correspond with current studies indicating that PVDF-based electrospun fibers have enhanced piezoelectric capabilities attributable to the high β-phase content of PVDF and the alignment of polymer chains generated by electrospinning, which improves charge generation and storage [40, 41]. The hydrogel alone demonstrates the lowest potential owing to its elevated water content and absence of conductive elements, while including HNT may facilitate minimal charge retention [22, 42]. The electrospun-hydrogel bilayer composite exhibits an intermediate V/g value, deriving advantages from the piezoelectric properties of the electrospun layer and the hydrogen bonding interactions in the hydrogel offer a promising hybrid system where electrospun fibers provide guidance cues for axonal growth. In contrast, the hydrogel enhances cell adhesion and nutrient diffusion.

Previous studies indicate that piezoelectric scaffolds with surface potentials around 0.8–1.2 V/g enhance neurogenesis and nerve cell adhesion [43, 44]. A bilayer polyurethane-collagen nerve conduit was reported to facilitate peroneal nerve regeneration, highlighting the importance of a bilayer structure in nerve repair, which aligned with this research outcome [45]. Overall, the electrospun-hydrogel bilayer composite presents the most suitable environment for nerve tissue

engineering, as it combines moderate conductivity, high porosity, and structural support, essential for nerve repair and regeneration. Optimizing fiber alignment, composite thickness, and hydrogel crosslinking could further enhance its bioelectrical and mechanical properties to match native nerve tissue better.

3.5 Biological Analysis

The biocompatibility and regenerative potential of the PVDF/PVA electrospun, PVA/Collagen/HNT hydrogel, and PVDF/PVA-PVA/Col/HNT bilayer scaffolds were evaluated using human fibroblast cells. Fibroblast cells are critical in preliminary studies assessing scaffolds for nerve tissue regeneration due to their role in wound healing, biocompatibility testing, cell proliferation, scaffold evaluation, and initial screening before using neuronal cells. They assess biocompatibility, toxicity, and fundamental cellular interactions, ensuring scaffolds are well-tested and optimized for their intended application in nerve tissue regeneration. The data was gathered using two key methods: the MTT assay, which measures cell metabolic activity as an indicator of viability (see Figure 5), and the Live-Dead Kit Assay, which assesses cell viability through fluorescent staining of live and dead cells (see Figure 6). The bilayer scaffold (PVDF/PVA-PVA/Col/HNT) demonstrated higher fibroblast cell viability (86.97%) than the single-layer scaffolds, correlating with its highest porosity (96.27%), which enhances cell infiltration, nutrient diffusion, and waste removal. The fiber diameter (165.7±0.4 nm) closely mimics the extracellular matrix, supporting better cell adhesion and neurite extension. Its lower surface roughness (R_a: 5.3 nm electrospun surface, 41.9 nm hydrogel surface) than PVDF/PVA electrospun (R_a: 192.5 nm) reduces excessive topographical barriers, improving cell spreading and attachment. These characteristics align with previous studies on bilayer scaffolds for tissue engineering, which report that optimized porosity, fiber morphology, and surface properties significantly enhance bioactivity and regenerative potential. The better integration of mechanical support from the PVDF/PVA layer and the hydrogel layer's biological compatibility seems to support higher initial cell activity. The Live-Dead Kit Assay result shown in Figure 6 confirms that the bilayer scaffold provides the best conditions for fibroblasts to grow and survive over time. This suggests that it has much potential for use in nerve regeneration.

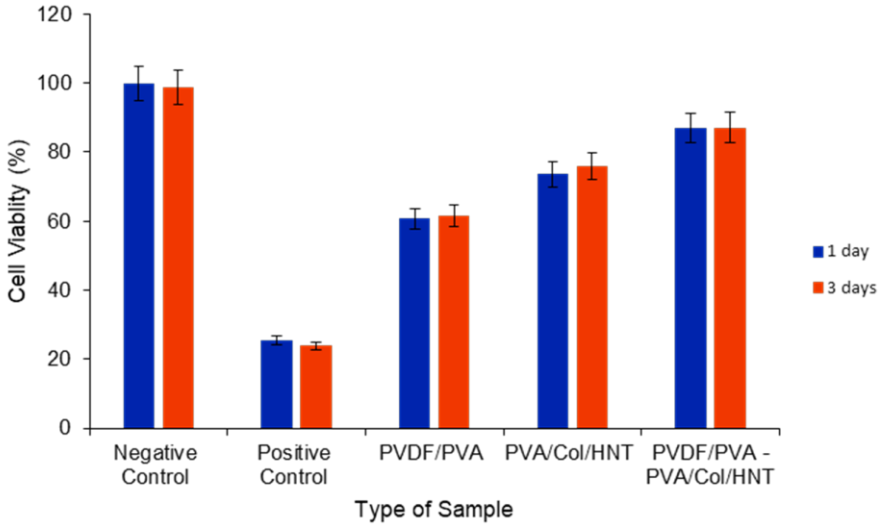

Figure 5. Cell viability percentage of the scaffolds after 1 and 3 days using MTT assay

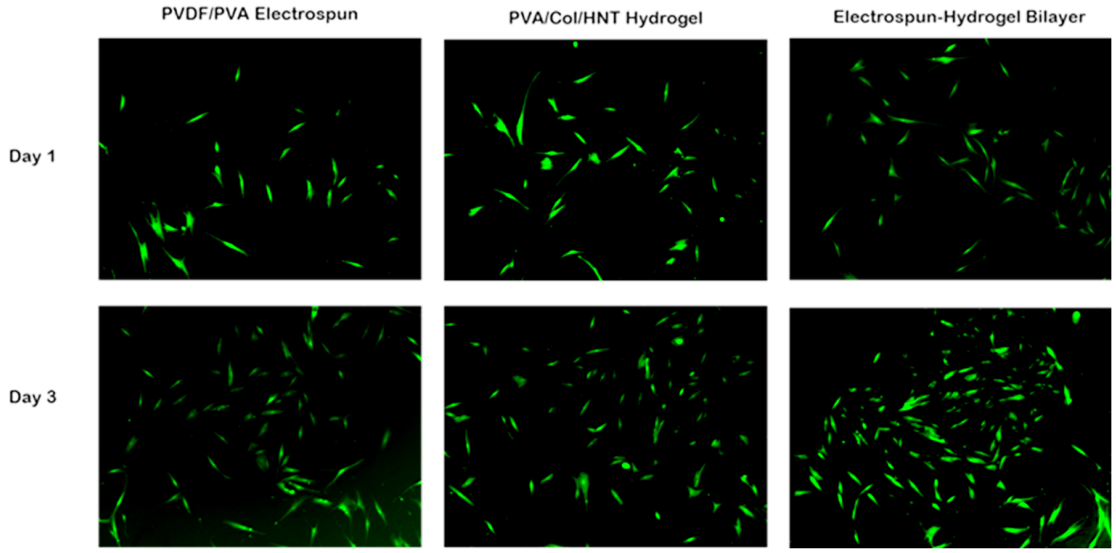

Figure 6. Cell viability images of the scaffold after 1 and 3 days using Live-Dead Kit assay

4. CONCLUSIONS

This study successfully fabricated and evaluated a bilayer scaffold composed of PVDF/PVA electrospun fibers and PVA/Collagen/HNT hydrogel for potential nerve tissue regeneration. FESEM micrographic analysis confirmed a uniform and interconnected structure, ensuring strong integration between the electrospun and hydrogel layers. Mechanical testing demonstrated that the bilayer scaffold exhibited enhanced mechanical properties, with increased tensile strength (1.762 MPa), Young's modulus (39.612 MPa), and elongation at break (316.253%), providing an optimal balance of structural integrity and flexibility—crucial for nerve regeneration applications. Surface roughness analysis revealed that the bilayer scaffold had significantly lower R_a values (5.3 nm electrospun surface, 41.9 nm hydrogel surface) than the single-layer electrospun mat (192.5 nm), facilitating better cell attachment and proliferation. Furthermore, conductivity analysis indicated an intermediate surface potential (0.892±0.1 V/g), benefiting from the piezoelectric properties of PVDF and hydrogen bonding interactions in the hydrogel, which aligns with the optimal range (0.8–1.2 V/g) for neurogenic stimulation and axonal growth guidance. FTIR analysis confirmed successful chemical interactions between the electrospun and hydrogel layers, ensuring structural stability and bioactivity. In vitro biocompatibility assays (MTT and Live-Dead Kit assays) using human fibroblast cells demonstrated significantly higher cell viability (86.97%) in the bilayer scaffold compared to single-layer scaffolds (PVDF/PVA: 60.66%, PVA/Col/HNT: 73.58%), indicating a highly conducive environment for cell proliferation and attachment. These findings highlight that the bilayer scaffold effectively integrates mechanical strength, bioactivity, and controlled conductivity, making it a promising candidate for nerve tissue engineering applications. Future studies should optimize fiber alignment, hydrogel crosslinking, and in vivo validation to enhance its neuro-regenerative potential further.

ACKNOWLEDGEMENTS

This research was funded by a Fundamental Research Grant Scheme (FRGS) FRGS/1/2022/TK09/UTHM/03/7 from the Ministry of Higher Education of Malaysia and Universiti Tun Hussein Onn Malaysia through Geran Penyelidikan Pascasiswazah (GPPS - H458).

CONFLICT OF INTEREST

The authors declare no conflicts of interest. There are no conflicts of interest with the submission of this manuscript, and all the writers have agreed that it can be published. This paper has not been published before, is not currently being reviewed by any other journal, and will not be sent anywhere else until this journal decides.

AUTHORS CONTRIBUTION

M. S. A. Hamzah (Conceptualization; Formal analysis; Investigation, writing)

N. H. M. Nayan (Conceptualization; Methodology; Review & Editing, Validation; Supervisions)

S. C. Fhoong (Methodology, Data Curation; Review)

N. Jusoh (Resources; Review; Validation)

AVAILABILITY OF DATA AND MATERIALS

The data supporting this study's findings are available on request from the corresponding author.

ETHICS STATEMENT

This study was conducted following ethical guidelines for in vitro research. All cell culture experiments complied with institutional biosafety regulations and standard laboratory protocols. No human or animal subjects were directly involved in this research, so ethical approval was not required. The authors declare no conflicts of interest related to this research.

REFERENCES

[1] G. Hussain, J. Wang, A. Rasul, H. Anwar, M. Qasim, S. Zafar, et al., "Current status of therapeutic approaches against peripheral nerve injuries: A detailed story from injury to recovery," *International Journal of Biological Sciences*, vol. 16, no. 1, pp. 116-134, 2020.

[2] C. R. Carvalho, R. L. Reis, J. M. Oliveira, "Fundamentals and current strategies for peripheral nerve repair and regeneration," *Advanced in Experimental Medicine and Biology*, vol. 1249, pp.173-201, 2020.

[3] M. E. Harley-Troxell, R. Steiner, R. C. Advincula, D. E. Anderson, M. Dhar, "Interactions of cells and biomaterials for nerve tissue Engineering: Polymers and fabrication," *Polymers*, vol. 15, no. 18, p. 3685, 2023.

[4] M. Miloro, G. E. Ghali, P. E. Larsen, P. Waite. Peterson's Principles of Oral and Maxillofacial Surgery. 4th Eds. Switzerland: Springer Cham, 2022.

[5] P. D. Dalton, K. L. O'Neill, A. P. Pêgo, G. W. Plant, D. R. Nisbet, M. Oudega, et al. Tissue Engineering of the Nervous System: Tissue Engineering. 3rd Eds. United States: Academic Press, 2023.

[6] N. Askarzadeh, M. H. Nazarpak, K. Mansoori, M. Farokhi, M. Gholami, J. Mohammadi, et al., "Bilayer cylindrical conduit consisting of electrospun polycaprolactone nanofibers and DSC cross-linked sodium alginate hydrogel to bridge peripheral nerve gaps," *Macromolecular Bioscience*, vol. 20, no. 9, p. 2000149, 2020.

[7] V, Pande, A. Kharde, P. Bhawar, V. Abhale, "Scaffolds: Porous scaffold for modulated drug delivery," *Austin Therapeutics*, vol. 3, no. 1, p. 1027, 2016.

[8] L. Yu, C. J. Bennett, C. H. Lin, S. Yan, J. Yang, "Scaffold design considerations for peripheral nerve regeneration," Journal of Neural Engineering, vol. 21, no. 4, p. 041001, 2024.

[9] J. Fang, L. Nan, K. Song, Z. Weng, J. Shan, V. Shahin, et al., "Application and progress of bionic scaffolds in nerve repair: A narrative review," *Advanced Technology in Neuroscience*, vol. 1, no. 1, pp. 43-50, 2024.

[10] M. Rahman, T. Mahady Dip, R. Padhye, S. Houshyar, "Review on electrically conductive smart nerve guide conduit for peripheral nerve regeneration," *Journal of Biomedical Materials Research Part A*, vol. 111, no. 12, pp. 1916-1950, 2023.

[11] Q. Wang, H. Wang, Y. Ma, X. Cao, H. Gao, "Effects of electroactive materials on nerve cell behaviors and applications in peripheral nerve repair," *Biomaterials Science*, vol. 10, no. 21, pp. 6061-6076, 2022.

[12] P. Saxena, P. Shukla, "A comprehensive review on fundamental properties and applications of poly (vinylidene fluoride) (PVDF)," *Advanced Composites and Hybrid Materials*, vol. 4, no. 1, pp. 8-26, 2021.

[13] Q. Li, C. Wen, J. Yang, X. Zhou, Y. Zhu, J. Zheng, et al., "Zwitterionic biomaterials," *Chemical Reviews*, vol. 122, no. 23, pp. 17073-17154, 2022.

[14] E. R. Radu, S. I. Voicu, V. K. Thakur, "Polymeric membranes for biomedical applications," *Polymers*, vol. 15, no. 3, p. 619, 2023.

[15] M. A. S. Hamzah, N. H. M. Nayan, N. Jusoh, "Optimization of polyvinylidene/polyvinyl alcohol electrospun using Taguchi method for tissue engineering application," *Journal of Advanced Research in Applied Mechanics*, vol. 15, no. 1, pp. 81-92, 2025.

[16] C. Bertsch, H. Maréchal, V. Gribova, B. Lévy, C. Debry, P. Lavalle, et al., "Biomimetic bilayered scaffolds for tissue engineering: from current design strategies to medical applications," *Advanced Healthcare Materials*, vol. 12, no. 17, p. 2203115, 2023.

[17] X. Yu, T. Zhang, Y. Li, "3D printing and bioprinting nerve conduits for neural tissue engineering," *Polymers*, vol. 12, no. 8, p. 1637, 2020.

[18] Y. Chen, Y. Xu, S. Ramakrishna, "Electromagnetic-responsive targeted delivery scaffold technology has better potential to repair injured peripheral nerves: A narrative review," *Advanced Technology in Neuroscience*, vol. 1, no. 1, pp. 51-71, 2024.

[19] S. H. Chen, P. H. Lien, F. H. Lin, P. Y. Chou, C. H. Chen, Z. Y. Chen, et al., "Aligned core–shell fibrous nerve wrap containing Bletilla striata polysaccharide improves functional outcomes of peripheral nerve repair," *International Journal of Biological Macromolecules*, vol. 241, p. 124636, 2023.

[20] M. S. A. Hamzah, N. H. M. Nayan, N. Jusoh, N. A. Maaruf, "Physiochemical and in-vitro bioactivity characterization of polyvinyl alcohol / halloysite nanotube / collagen (PVA/HNT/Col) using freeze-thawing method and spin coated technique for wound healing applications," *Journal of Advanced Research in Applied Mechanics*, vol. 152, no. 1, pp. 68-80, 2025.

[21] ASTM E2859-11, "Standard Guide for Size Measurement of Nanoparticles Using Atomic Force Microscopy," *American Society for Testing and Materials*, United States, 2023.

[22] ASTM D3039/D3039M, "Standard Test Method for Tensile Properties of Polymer Matrix Composite Materials," *American Society for Testing and Materials*, United States, 2023.

[23] H. Gade, N. Parsa, O. S. Roberts, G. G. Chase, D. H. Reneker, "Charge measurement of electrospun polyvinylidene fluoride fibers using a custom-made Faraday bucket," *Review of Scientific Instruments*, vol. 91, no. 7, p. 0075107, 2020.

[24] H. Gade, S. Nikam, G. G. Chase, D. H. Reneker, "Effect of electrospinning conditions on β-phase and surface charge potential of PVDF fibers," *Polymer*, vol. 228, p.123902, 2021.

[25] G. G. Flores-Rojas, B. Gómez-Lazaro, F. López-Saucedo, R. Vera-Graziano, E. Bucio, E. Mendizábal, "Electrospun scaffolds for tissue engineering: A review," *Macromol*, vol. 3, no. 3, pp. 524-553, 2023.

[26] J. M. Ameer, A. K. Pr, N. Kasoju, "Strategies to tune electrospun scaffold porosity for effective cell response in tissue engineering," *Journal of Functional Biomaterials*, vol. 10, no. 3, p. 30, 2019.

[27] D. Wang, J. Wu, S. Wu, X. Chen, W. Li, X. Chen, et al., "Ice-mediated reactions and assemblies in diverse domains," *Advanced Functional Materials*, vol. 34, no. 29, p. 2315532, 2024.

[28] B. He, S. Ding, Z. Shi, "A comparison between profile and areal surface roughness parameters," *Metrology and Measurement Systems*, vol. 28, no. 3, pp. 413-438, 2021.

[29] M. J. Woźniak, A. Chlanda, P. Oberbek, M. Heljak, K. Czarnecka, M. Janeta, et al., "Binary bioactive glass composite scaffolds for bone tissue engineering—Structure and mechanical properties in micro and nano scale. A preliminary study," *Micron*, vol. 119, pp. 64-71, 2019.

[30] I. Sands, R. Demarco, L. Thurber, A. Esteban-Linares, D. Song, E. Meng, et al., "Interface-mediated neurogenic signaling: The impact of surface geometry and chemistry on neural cell behavior for regenerative and brain–machine interfacing applications," *Advanced Materials*, vol. 36, no. 33, p. 2401750, 2024.

[31] Y. Qian, H. Lin, Z. Yan, J. Shi, C. Fan, "Functional nanomaterials in peripheral nerve regeneration: Scaffold design, chemical principles and microenvironmental remodeling," *Materials Today*, vol. 51, pp. 165-187, 2021.

[32] N. Ghane, M. H. Beigi, S. Labbaf, M. H. Nasr-Esfahani, A. Kiani, "Design of hydrogel-based scaffolds for the treatment of spinal cord injuries," *Journal of Materials Chemistry B*, vol. 8, no. 47, pp. 10712-10738, 2020.

[33] G. Kazemzadeh, N. Jirofti, H. K. Mehrjerdi, M. Rajabioun, S. A. Alamdaran, D. Mohebbi-Kalhori, et al., "A review on developments of in-vitro and in-vivo evaluation of hybrid PCL-based natural polymers nanofibers scaffolds for vascular tissue engineering," *Journal of Industrial Textiles*, vol. 52, pp. 1-26, 2022.

[34] E. Tanzli, A. Ehrmann, "Electrospun nanofibrous membranes for tissue engineering and cell growth," *Applied Sciences*, vol. 11, no. 15, p. 6929, 2021.

[35] A. K. Kolour, S. Ghoraishizadeh, M. S. Zaman, A. Alemzade, M. Banavand, J. Esmaeili, et al., "Janus films wound dressing comprising electrospun gelatin/PCL nanofibers and gelatin/honey/curcumin thawed layer," *ACS Applied Bio Materials*, vol. 7, no. 12, pp. 8642-8655, 2024.

[36] M. D. M. C. Delgado, "Electrospun functional nanofibers for antimicrobial applications in air filtration and wound dressing," *Ph.D. Thesis*, Hong Kong University of Science and Technology, Hong Kong, 2022.

[37] M. Andonegi, D. Correia, N. Pereira, M. Salado, C. M. Costa, S. Lanceros-Mendez, et al., "Sustainable collagen blends with different ionic liquids for resistive touch sensing applications," *ACS Sustainable Chemistry & Engineering*, vol. 11, no. 15, pp. 5986-5998, 2023.

[38] M. O. Yusuf, "Bond characterization in cementitious material binders using Fourier-transform infrared spectroscopy," *Applied Sciences*, vol. 13, no. 5, p. 3353, 2023.

[39] S. A. Bernal-Chávez, A. Romero-Montero, H. Hernández-Parra, S. I. Peña-Corona, M. L. Del Prado-Audelo, S. Alcalá-Alcalá, et al., "Enhancing chemical and physical stability of pharmaceuticals using freeze-thaw method: challenges and opportunities for process optimization through quality by design approach," *Journal of Biological Engineering*, vol. 17, no. 1, p. 35, 2023.

[40] M. Zhang, C. Liu, B. Li, Y. Shen, H. Wang, K. Ji, et al., "Electrospun PVDF-based piezoelectric nanofibers: materials, structures, and applications," *Nanoscale Advances*, vol. 5, no. 4, pp. 1043-1059, 2023.

[41] G. Kalimuldina, N. Turdakyn, I. Abay, A. Medeubayev, A. Nurpeissova, D. Adair, et al., "A review of piezoelectric PVDF film by electrospinning and its applications," *Sensors*, vol. 20, no. 18, p. 5214, 2020.

[42] E. Gkouma, E. Gianni, K. Avgoustakis, D. Papoulis, "Applications of halloysite in tissue engineering," *Applied Clay Science*, vol. 214, p. 106291, 2021.

[43] V. A. Revkova, K. V. Sidoruk, V. A. Kalsin, P. A. Melnikov, M. A. Konoplyannikov, S. Kotova, et al., "Spidroin silk fibers with bioactive motifs of extracellular proteins for neural tissue engineering," *ACS Omega*, vol. 6, no. 23, pp. 15264-15273, 2021.

[44] C. H. Cheng, W. C. Chen, W. C., Yang, S. C. Yang, S. M. Liu, Y. S. Chen, et al., "Unidirectional polyvinylidene/copper-impregnated nanohydroxyapatite composite membrane prepared by electrospinning with piezoelectricity and biocompatibility for potential ligament repair," *Polymers*, vol. 17, no. 2, p.185, 2025.

[45] S. T. Nasab, N. H. Roodbari, V. Goodarzi, H. A. Khonakdar, M. R. Nourani, "Nanobioglass enhanced polyurethane/collagen conduit in sciatic nerve regeneration" *Journal of Biomedical Materials Research Part B: Applied Biomaterials*, vol. 110, no. 5, pp. 1093-1102, 2022.